J|A|C|S ARTICLES

Published on Web 09/27/2010

Alternating Covalent Bonding Interactions in a One-Dimensional Chain of a Phenalenyl-Based Singlet Biradical Molecule Having Kekulé Structures

Akihiro Shimizu,[†] Takashi Kubo,*[,†] Mikio Uruichi,[‡] Kyuya Yakushi,[‡] Masayoshi Nakano,[§] Daisuke Shiomi,[||] Kazunobu Sato,[||] Takeji Takui,[||] Yasukazu Hirao,[†] Kouzou Matsumoto,[†] Hiroyuki Kurata,[†] Yasushi Morita,[†] and Kazuhiro Nakasuji[†]

Department of Chemistry, Graduate School of Science, Osaka University, Toyonaka, Osaka 560-0043, Japan, Institute for Molecular Science, Okazaki, Aichi 444-8585, Japan, Department of Materials Engineering Science, Graduate School of Engineering Science, Osaka University, Toyonaka, Osaka 560-8531, Japan, and Department of Chemistry and Material Science, Graduate School of Science, Osaka City University, Sumiyoshi-ku, Osaka 558-8585, Japan

Received October 13, 2009; E-mail: kubo@chem.sci.osaka-u.ac.jp

Abstract: A novel naphthoquinoid singlet biradical (**2a**) stabilized by phenalenyl rings is prepared by a multistep procedure and is investigated in terms of covalent bonding interactions. The molecule **2a** gives single crystals, in which a 1D chain is formed with a very short $\pi-\pi$ contact at the overlapping phenalenyl rings. The unpaired electrons in **2a** are involved in covalent bonding interactions not only within the molecule but also between the molecules in the 1D chain, and a linear conjugation is made of the alternating intra- and intermolecular covalent bonding interactions through conventional π-conjugation and multicenter bonding, respectively. The linear conjugation causes a lower-energy shift of the optical transition band in the crystal, but the transition energy is higher than that of the benzoquinoid singlet biradical (**1a**). This optical behavior and the magnetic susceptibility measurements reveal that the intermolecular covalent bonding interaction in the 1D chain of **2a** is greater in strength than the intramolecular one, despite the fact that a fully conjugated Kekulé structure can be drawn for **2a**.

Introduction

Quinoid hydrocarbons have attracted the continuous attention of chemists with their unusual reactivity and electronic structure derived from a small HOMO−LUMO energy gap.[1] The simplest representatives, *o*- and *p*-quinodimethane, have been the most extensively studied by chemical,[2] spectroscopic,[3] and theoretical[4] methods, which illuminate the nature of a biradical with a singlet ground state. π-Extended quinodimethanes such as Chichibabin's hydrocarbon,[5] cyclohepta[*def*]fluorene,[6] and polyacenes[7] (Chart 1) and nanographenes[8] have also been discussed in terms of their biradical nature. One of the fundamental issues of Kekulé compounds having biradical nature would concern the spin structure of their ground state, but it has been a formidable task to experimentally characterize the structure as in the case of a long history of Chichibabin's hydrocarbon. Such species possess the characteristic electronic structure that two electrons on the radical centers in their biradical canonical forms are weakly coupled within the molecule, and the case of adequately weak coupling finds the species bearing singlet biradical character. Because of the open-shell character, most

Chart 1

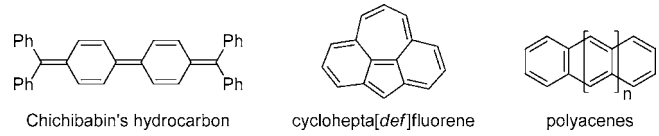

Chichibabin's hydrocarbon cyclohepta[*def*]fluorene polyacenes

[†] Graduate School of Science, Osaka University.
[‡] Institute for Molecular Science.
[§] Graduate School of Engineering Science, Osaka University.
[||] Osaka City University.

(1) Platz, M. S. Quinodimethanes and Related Diradicals. In *Diradicals*; Borden, W. T., Ed.; John Wiley & Sons: New York, 1982; Chapter 5.
(2) A series of "The Chemistry of Xylylenes" is reported by Errede. See: Errede, L. A.; English, W. D. *J. Org. Chem.* **1963**, *28*, 2646–2649, and references cited therein.
(3) ^{1}H-NMR spectroscopy: (a) Williams, D. J.; Pearson, J. M.; Levy, M. *J. Am. Chem. Soc.* **1970**, *92*, 1436–1438. (b) Trahanovsky, W. S.; Lorimor, S. P. *J. Org. Chem.* **2006**, *71*, 1784–1794. (c) Pearson, J. M.; Six, H. A.; Williams, D. J.; Levy, M. *J. Am. Chem. Soc.* **1971**, *93*, 5034–5036. (d) Flynn, C. R.; Michl, J. *J. Am. Chem. Soc.* **1974**, *96*, 3280–3288. IR and Raman: (e) Yamakita, Y.; Furukawa, Y.; Tasumi, M. *Chem. Lett.* **1993**, 311–314. (f) Yamakita, Y.; Tasumi, M. *J. Phys. Chem.* **1995**, *99*, 8524–8534. (g) Tseng, K. L.; Michl J., *J. Am. Chem. Soc.* **1977**, *99*, 4840–4842. Photoelectron: (h) Koenig, T.; Wielesek, R.; Snell, W.; Balle, T. *J. Am. Chem. Soc.* **1975**, *97*, 3225–3226.
(4) Döhnert, D.; Koutecký, J. *J. Am. Chem. Soc.* **1980**, *102*, 1789–1796.
(5) Montgomery, L. K.; Huffman, J. C.; Jurczak, E. A.; Grendze, M. P. *J. Am. Chem. Soc.* **1986**, *108*, 6004–6011, and references cited therein.
(6) Grieser, U.; Hafner, K. *Chem. Ber.* **1994**, *127*, 2307–2314.
(7) Bendikov, M.; Duong, H. M.; Starkey, K.; Houk, K. N.; Carter, E. A.; Wudl, F. *J. Am. Chem. Soc.* **2004**, *126*, 7416–7417.
(8) (a) Fujita, M.; Wakabayashi, K.; Nakada, K.; Kusakabe, K. *J. Phys. Soc. Jpn.* **1996**, *65*, 1920–1923. (b) Jian, D.; Sumpter, B. G.; Dai, S. *J. Chem. Phys.* **2007**, *127*, 124703−1–5.

Scheme 1. Resonance Structures of **1** and **2**[a]

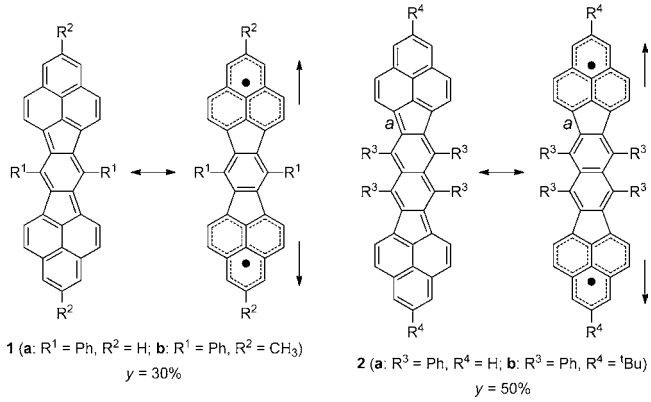

[a] Amounts of biradical character (*y*) were calculated with a CASSCF(2,2)/6-31G//RB3LYP/6-31G** method.

singlet biradical species are short-lived, and this high reactivity obscures the identification of spin structure and characteristic functional properties. However, recent progress in stable singlet biradicals provides the opportunity to examine them precisely by using various analytical methods.[9]

In the course of our studies on stable singlet biradicals, we have investigated benzoquinoid hydrocarbons (**1a** and **1b**), which are thermodynamically stabilized by exploiting the spin-delocalizing character of phenalenyl radical, as shown in Scheme 1, showing that in the crystal, **1a** and **1b** form $\pi-\pi$ one-dimensional (1D) chains with very short $\pi-\pi$ separation distances between the overlapping phenalenyl rings.[10] In the 1D chain, electrons of the singlet biradicals are involved in covalent bonding interactions not only within the molecule but also between the molecules. Furthermore, the sterically perturbed molecule **1b** gave many polymorphic crystals, in which various separation distances (including nonoverlapping) were observed depending on experimental conditions.[10b] The changes in the separation distances varied the intermolecular covalent bonding interaction in magnitude in the 1D chain, and consequently a peak shift was observed in their reflection spectra. Thus, both the intra- and intermolecular covalent bonding interactions play a key role in the singlet-biradical-based molecular properties or material functionalities.

In this paper, we report the synthesis, crystal packing, and covalent bonding interactions of a phenalenyl-based naphthoquinoid hydrocarbon **2a** whose ground state is also described in terms of the resonance of Kekulé and biradical structures. Our previous study of di-*tert*-butyl derivative **2b** has demonstrated that the intramolecular covalent bonding interaction is weakened compared with that in **1**; the reason is that the expansion of the central π-system from benzoquinoid to naphthoquinoid structure increases the biradical contribution in the ground state.[11] We focus our attention for **2a** on the effect of larger biradical character on the solid state properties such as overlapping structures of phenalenyl rings, optical transition in a crystal, magnetic properties, and electroconductivity.

Results and Discussion

Theoretical Consideration of Biradical Character. The hydrocarbon **2** consists of 2,6-naphthoquinodimethane and two phenalenyl moieties. The quinoid Kekulé structure of **2** resonates well with a biradical structure, because the formal double bond loss in the biradical structure is compensated with aromatic stabilization energy of the central naphthalene ring. Considering the extent of the aromatic stabilization energy of benzene and naphthalene, **2** owns a larger contribution of the biradical structure in the ground state than **1**.

As mentioned above, quinoid compounds encounter difficulty in the experimental elucidation of their biradical character. Instead, a theoretical study gives an obvious criterion,[12] and the amount of the biradical character is estimated by the natural orbital occupation number (NOON).[4] In a multiconfigurational scheme, the mixing of a doubly excited configuration, $^1\Phi_{H,H\rightarrow L,L}$, with a ground state configuration, $^1\Phi_{H,H}$, represents uncoupling of an electron pair, and hence the occupation number of the LUMO is a direct computational measure of the amount of biradical character. A perfect biradical is characterized by occupation numbers of 1.0 in HOMO and LUMO, whereas a perfect closed-shell molecule possesses occupation numbers of 2.0 and 0.0 in HOMO and LUMO, respectively. We performed a CASSCF(2,2)/6-31G//RB3LYP/6-31G** calculation for **1** and **2**, which gave LUMO occupation numbers of 0.30 and 0.50, and consequently the amounts of the biradical character were estimated to be 30% and 50%, respectively. A UHF-based broken symmetry method gives another quantitative guidance for the biradical character.[13] A broken-symmetry UB3LYP/6-31G** calculation of **1** and **2** gave LUMO occupation numbers of 0.37 and 0.56 with spin contaminations $\langle S^2\rangle = 0.65$ and 0.87, respectively. Spin densities on the phenalenyl rings are larger for **2** than for **1** as listed in Table 1. These quantum chemical calculations indicate more enhanced biradical character for **2** and are thoroughly consistent with the Kekulé formula consideration relevant to the biradical character described above.

The very large biradical character of **2** is associated with a weak coupling of two unpaired electrons on the phenalenyl rings through the naphthalene linker. With the help of a perturbation MO analysis,[14] the nonbonding singly occupied MO (SOMO)

(9) (a) Herebian, D.; Wieghardt, K. E.; Neese, F. *J. Am. Chem. Soc.* **2003**, *125*, 10997–11005. (b) Ziessel, R.; Stroh, C.; Heise, H.; Köhler, F. H.; Turek, P.; Claiser, N.; Souhassou, M.; Lecomte, C. *J. Am. Chem. Soc.* **2004**, *126*, 12604–12613. (c) Rodriguez, A.; Olsen, R. A.; Ghaderi, N.; Scheschkewitz, D.; Tham, F. S.; Mueller, L. J.; Bertrand, G. *Angew. Chem., Int. Ed.* **2004**, *43*, 4880–4883. (d) Porter III, W. W.; Vaid, T. P.; Rheingold, A. L. *J. Am. Chem. Soc.* **2005**, *127*, 16559–16566. (e) Hiroto, S.; Furukawa, K.; Shinokubo, H.; Osuka, A. *J. Am. Chem. Soc.* **2006**, *128*, 12380–12381. (f) Casado, J.; Patchkovskii, S.; Zgierski, M. Z.; Hermosilla, L.; Sieiro, C.; Oliva, M. M.; Navarrete, J. T. L. *Angew. Chem., Int. Ed.* **2008**, *47*, 1443–1446. (g) Ueda, A.; Nishida, S.; Fukui, K.; Ise, T.; Shiomi, D.; Sato, K.; Takui, T.; Nakasuji, K.; Morita, Y. *Angew. Chem., Int. Ed.* **2010**, *49*, 1678–1682. (h) Kamada, K.; Ohta, K.; Kubo, T.; Shimizu, A.; Morita, Y.; Nakasuji, K.; Kishi, R.; Ohta, S.; Furukawa, S.-I.; Takahashi, H.; Nakano, M. *Angew. Chem., Int. Ed.* **2007**, *46*, 3544–3546. (i) Kamada, K.; Ohta, K.; Shimizu, A.; Kubo, T.; Kishi, R.; Takahashi, H.; Botek, E.; Champagne, B.; Nakano, M. *J. Phys. Chem. Lett.* **2010**, *1*, 937–940.

(10) (a) Kubo, T.; Shimizu, A.; Sakamoto, M.; Uruichi, M.; Yakushi, K.; Nakano, M.; Shiomi, D.; Sato, K.; Takui, T.; Morita, Y.; Nakasuji, K. *Angew. Chem., Int. Ed.* **2005**, *44*, 6564–6568. (b) Shimizu, A.; Uruichi, M.; Yakushi, K.; Matsuzaki, H.; Okamoto, H.; Nakano, M.; Hirao, Y.; Matsumoto, K.; Kurata, H.; Kubo, T. *Angew. Chem., Int. Ed.* **2009**, *48*, 5482–5486.

(11) Kubo, T.; Shimizu, A.; Uruichi, M.; Yakushi, K.; Nakano, M.; Shiomi, D.; Sato, K.; Takui, T.; Morita, Y.; Nakasuji, K. *Org. Lett.* **2007**, *9*, 81–84.

(12) (a) Salem, L.; Rowland, C. *Angew. Chem., Int. Ed. Engl.* **1972**, *11*, 92–111. (b) Bonačić-Koutecký, V.; Koutecký, J.; Michl, J. *Angew. Chem., Int. Ed. Engl.* **1987**, *26*, 170–189.

(13) (a) Noodleman, L. *J. Chem. Phys.* **1981**, *74*, 5737–5743. (b) Yamaguchi, K. *Chem. Phys. Lett.* **1975**, *33*, 330–335.

(14) Dewar, M. J. S.; Dougherty, R. C. *The PMO Theory of Organic Chemistry*; Plenum Press: New York, 1975.

Table 1. Spin Densities (ρ) on the Carbon Atoms[a] of **1** and **2** Calculated with a Broken-Symmetry UB3LYP/6-31G** Method

1		2	
positions	ρ	positions	ρ
1, 3	−0.202	1, 3	−0.229
2	+0.100	2	+0.114
3a, 16a	+0.094	3a, 18a	+0.107
4, 16	−0.213	4, 18	−0.241
5, 15	+0.110	5, 17	+0.124
5a, 14b	−0.218	5a, 16b	−0.248
5b, 14a	+0.030	5b, 16a	+0.048
6, 14	0.000	6, 16	−0.061
6a, 13b	−0.030	6a, 15a	0.000
6b, 13a	+0.218	7, 15	+0.061
7, 13	−0.110	7a, 14b	−0.048
8, 12	+0.213	7b, 14a	+0.248
8a, 11a	−0.094	8, 14	−0.124
8b	+0.048	9, 13	+0.241
8c	−0.096	9a, 12a	−0.107
9, 11	+0.202	9b	+0.056
10	−0.100	9c	−0.111
16b	−0.048	10, 12	+0.229
16c	+0.096	11	−0.114
		18b	−0.056
		18c	+0.111

[a] Atom positions are shown in the following drawings:

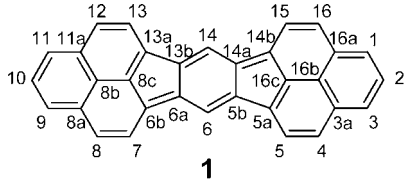

1

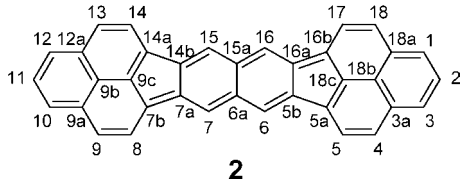

2

of phenalenyl radical is weakly perturbed by the MOs of naphthalene, because the aromatic character of naphthalene serves a wide energy gap between the bonding and antibonding orbitals and hence the MOs of both fragments differ considerably in energy. Thus, the mixing of the phenalenyl's SOMO with the naphthalene's MOs is not effective, and the HOMO and LUMO of **2** retain the character of the SOMO of phenalenyl radical as shown in Figure 1. For this reason, **2** has a small energy gap as well as a large spatial overlap between the HOMO and LUMO, which are favorable for the mixing of $^1\Phi_{H,H\rightarrow L,L}$ with $^1\Phi_{H,H}$. The small HOMO−LUMO energy gap of **2** has been confirmed by the cyclic voltammetry measurement of **2b**, which gives ΔE^{redox} ($= E^{ox} - E^{red}$) of 1.04 V.[11]

Synthesis. The synthetic procedure for **2a** is outlined in Scheme 2. The starting material **3** was synthesized according to the previously reported procedures[15,11] and was converted to dibromo derivatives **4** as a mixture of 3,11- and 3,12-isomers. The individual isomers were not isolated because both compounds were expected to lead to a single compound **2a**. Heck reaction of **4** with methyl acrylate and subsequent hydrogenation of the alkenes **5** afforded ester compounds **6**. Hydrolysis of **6**

(15) Neudorff, W. D.; Schulte, N.; Lentz, D.; Schlüter, A. D. *Org. Lett.* **2001**, *3*, 3115–3118.

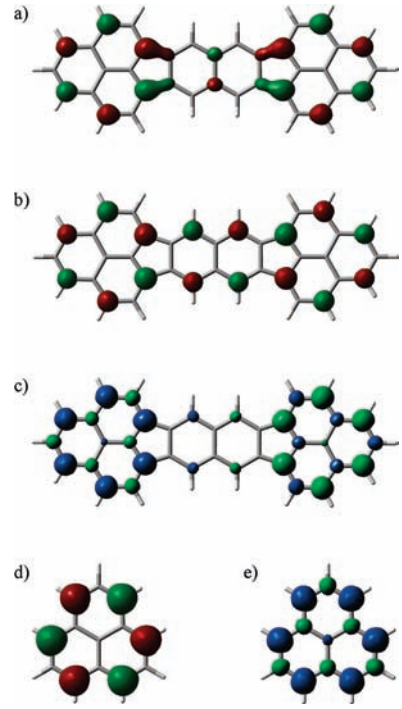

Figure 1. (a) HOMO, (b) LUMO, and (c) spin densities of **2** and (d) SOMO and (e) spin densities of phenalenyl radical. The calculations are performed at RB3LYP/6-31G** (a, b) and UB3LYP/6-31G** (c, d, e) levels of theory. Blue and green surfaces of the spin density maps represent α and β spin densities, respectively, drawn at 0.004 e/au^3 level.

Scheme 2. Synthesis of **2a**[a]

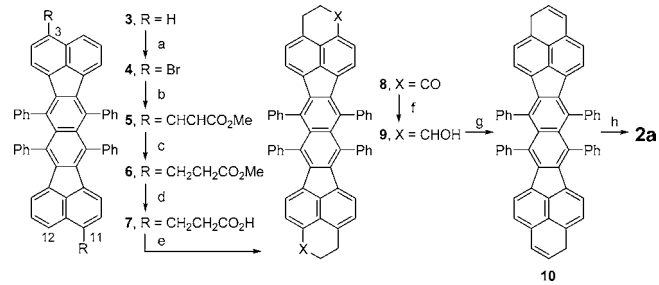

[a] Reaction conditions: (a) Br_2, CH_2Cl_2, rt, 92%; (b) $CH_2{=}CHCO_2CH_3$, $Pd(CH_3CN)_2Cl_2$, Ph_4PCl, AcONa, DMF, 140 °C; (c) Zn, AcOH, toluene, reflux, 71% (2 steps); (d) LiI, 2,4,6-trimethylpyridine, 185 °C; (e) $(COCl)_2$, reflux, then $AlCl_3$, CH_2Cl_2, −78 to −30 °C, 71% (2 steps); (f) $NaBH_4$, CH_2Cl_2, EtOH, rt, 100%; (g) TsOH·H_2O, toluene, 90 °C, 87%; (h) *p*-chloranil, benzene, reflux, 83%.

gave carboxylic acid derivatives **7**. Intramolecular Friedel−Crafts cyclization of acyl chloride of **7** with $AlCl_3$ gave diketones **8**, which were reduced with $NaBH_4$ and subsequently dehydrated with TsOH to afford dihydro compounds **10**. Finally **10** was dehydrogenated with *p*-chloranil to give **2a**. Due to the extremely low solubility, recrystallization of the crude material **2a** failed. Instead, by cooling the reaction mixture in the final dehydrogenation step, we successfully obtained single crystals of **2a** as dark purple plates. The solid **2a** was found to be stable at room temperature in air for a couple of days.

Molecular Geometry. The X-ray crystallographic analysis of **2a** at 200 K revealed effective D_{2h} symmetry for the main core ring. The four phenyl rings were nearly perpendicular to the main core ring because of steric crowding (Figure 2). In the crystal, **2a** formed a 1D chain in a slipped stack arrangement running parallel to the (0 0 1) plane (Figure 3 and Supporting Information, Figure S1).

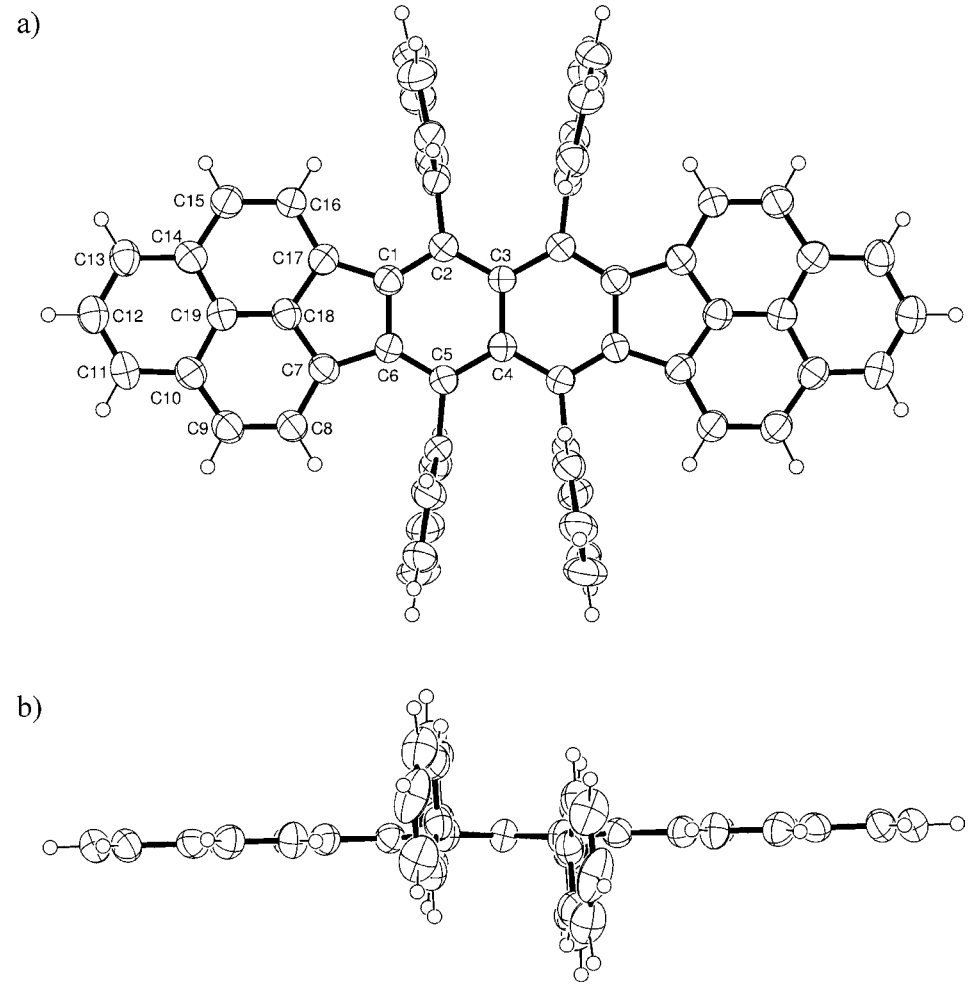

Figure 2. ORTEP drawings of **2a** at 200 K: (a) top view and (b) side view. Displacement ellipsoids are drawn at the 50% probability level.

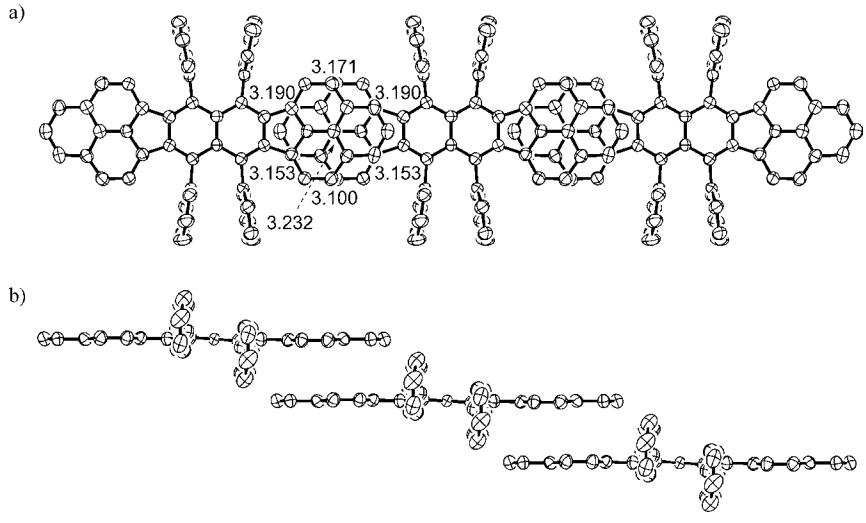

Figure 3. (a) Top view and (b) side view of the 1D chain of **2a** at 200 K. Hydrogen atoms are omitted for clarity. In the top view, distances of the short C−C contact in the overlapping phenalenyl rings are also shown.

The crystal structure of **2a** contains two salient features: (1) **2a** reproduces the superimposed phenalenyl overlap that is almost identical to that of **1a**, and (2) the phenalenyl rings of **2a** retain the π-dimeric structure of the phenalenyl radical,[16] not the σ-dimer, despite the fact that the spin densities on the phenalenyl rings are larger than those of **1a**. Both the $\pi-\pi$ separation distance (3.170 Å for **2a**, 3.137 Å for **1a**) and the overlapping mode of the phenalenyl rings are similar, strongly suggesting that the most dominant interaction controlling the crystal packing of **2a** as well as **1a** is the intermolecular bonding interaction due to the phenalenyl overlap. Recently the bonding interaction in a π-dimer of phenalenyl radical itself has been referred to as multicenter bonding,[17] which has attracted attention as a new type of chemical bond. A dominant attractive

force in the multicenter bonding is the dispersion force, whereas a covalent bonding interaction is also operative due to a large SOMO−SOMO overlap, leading to the $\pi-\pi$ overlap at a distance less than the sum of the van der Waals radius of the carbon atom. In the phenalenyl overlap of **2a**, the distances of the seven short-contact pairs of carbon atoms are much less than the sum of the van der Waals radius of carbon atom (Figure 3a), and furthermore, the peripheral α-carbons,[18] which bear large spin densities, show shorter contacts than the central carbon (C19 in Figure 2a) with no spin density. This overlapping pattern suggests the appreciable intermolecular covalent bonding interaction, as demonstrated in the recent theoretical study by Kertesz.[17d]

The larger spin densities on the phenalenyl rings of **2a** than those of **1a** should give a more enhanced attractive force in the phenalenyl overlap and, naturally, would reduce the $\pi-\pi$ separation distance. However, the distance found in **2a** was slightly larger than that of **1a**. Head-Gordon et al. performed a CP-MRMP2 calculation to estimate the potential energy surface of the phenalenyl radical π-dimer itself as a function of the separation distance and found a global minimum for the geometry at the distance of around 3.1 Å.[19] The potential energy surface is relatively shallow at the minimum point, and the phenalenyl radical π-dimer can take various separation distances with only small changes in total energy, whereas the potential energy increases steeply with the distance decreasing below 3.0 Å. This theoretical finding indicates that the attractive forces of the intermolecular covalent bonding interaction as well as dispersion are well balanced against an interatomic repulsion at the separation distance of ∼3.1 Å. Therefore, a stronger intermolecular covalent bonding interaction in the 1D chain of **2a** does not necessarily give a shorter separation distance.

Here, we should consider a C−C σ-bond formation, which most organic radicals experience. Actually phenalenyl radical has a more stabilized dimeric structure, σ-dimer, which is supported experimentally[20] and theoretically.[21] Preference of the π-dimeric structure in **2a** indicates that there is still an adequate intramolecular bonding interaction of electrons through the naphthalene linker so as to reduce the spin densities on the phenalenyl rings. Considering the condition-dependent π-/σ-dimerization of a spirobiphenalenyl radical (octyl derivative),[22] the actual spin densities of **2a** on the phenalenyl rings can be comparable to or less than those of the spirobiphenalenyl system, which are almost half of those of phenalenyl radical itself.

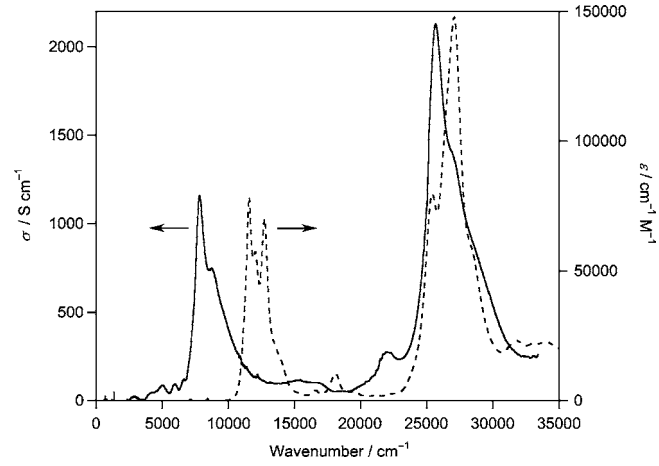

Figure 4. Optical conductivity of **2a** obtained with light on the (0 0 1) surface (solid line) and absorption spectrum of **2b** in hexane−CH_2Cl_2 (dashed line).

The covalent bonding interaction between the molecules would affect the strength of the intramolecular covalent bonding interaction. We focus on the length of the bonds denoted by *a* of **2** in Scheme 1, which connect the phenalenyl rings and the naphthalene ring, because the bond length is the most sensitive to the contribution weight of each canonical structure in the resonance formula (the bond *a* has the bond order of 1.5 in the Kekulé structure, whereas single bond character in the biradical structure). The length of the bond *a* of **2a** is longer (1.471(5) Å) than that of **2b** (1.465(7) Å),[11] suggesting that the covalent bonding interaction between the molecules weakens the intramolecular one in **2a**.[23] Similar behavior has been observed in **1b** when the separation distance between the phenalenyl rings is altered with various temperatures.[10b] On the other hand, the bond length of **2a** is shorter than the length of the corresponding bond in 7,16-diphenylfluorantheno[8,9-*k*]fluoranthene (1.481(2) Å),[15] suggesting that **2a** still has the adequate covalent bonding interaction within the molecule.

Optical Property. Unlike usual intermolecular attractive forces such as electrostatic, polarization, and dispersion, the multicenter bonding mostly contributes to a large orbital overlap between molecules, because the multicenter bonding involves in-phase bonding interaction of partially occupied molecular orbitals. In the case of **1a** and **1b**, strong covalent bonding interactions of electrons through the multicenter bonding as well as conventional intramolecular π-conjugation have resulted in linear conjugation in their 1D chains, and consequently the lower-energy shifts of HOMO−LUMO bands are observed.[10]

A similar shift was also observed for **2a** in the solid state. Figure 4 shows the optical conductivity of a single crystal of **2a** along with the solution spectrum of **2b**.[24] The optical conductivity spectrum, which was obtained by the Kramers−Kronig transformation of the reflection spectrum measured with light

(16) Goto, K.; Kubo, T.; Yamamoto, K.; Nakasuji, K.; Sato, K.; Shiomi, D.; Takui, T.; Kubota, M.; Kobayashi, T.; Yakusi, K.; Ouyang, J. *J. Am. Chem. Soc.* **1999**, *121*, 1619–1620. For a recent review, see: Morita, Y.; Nishida, S. In *Stable Radicals: Fundamental and Applied Aspects of Odd-electron Compounds*; Hicks, R., Ed.; Wiley-Blackwell: New York, 2010; Chapter 3.

(17) (a) Suzuki, S.; Morita, Y.; Fukui, K.; Sato, K.; Shiomi, D.; Takui, T.; Nakasuji, K. *J. Am. Chem. Soc.* **2006**, *128*, 2530–2531. (b) Mota, F.; Miller, J. S.; Novoa, J. J. *J. Am. Chem. Soc.* **2009**, *131*, 7699–7707. (c) Tian, Y.-H.; Huang, J.; Kertesz, M. *Phys. Chem. Chem. Phys.* **2010**, *12*, 5084–5093. (d) Tian, Y.-H.; Kertesz, M. *J. Am. Chem. Soc.* **2010**, *132*, 10648–10649.

(18) The carbon atoms of phenalenyl bearing a large coefficient in SOMO are referred to as the α-carbon.

(19) Small, D.; Zaitsev, V.; Jung, Y.; Rosokha, S. V.; Head-Gordon, M.; Kochi, J. K. *J. Am. Chem. Soc.* **2004**, *126*, 13850–13858.

(20) (a) Reid, D. H. *Q. Rev., Chem. Soc.* **1965**, *19*, 274–302. (b) Gerson, F. *Helv. Chim. Acta* **1966**, *49*, 1463–1467. (c) Zaitsev, V.; Rosokha, S. V.; Head-Gordon, M.; Kochi, J. K. *J. Org. Chem.* **2006**, *71*, 520–526.

(21) Small, D.; Rosokha, S. V.; Kochi, J. K.; Head-Gordon, M. *J. Phys. Chem. A* **2005**, *109*, 11261–11267.

(22) Liao, P.; Itkis, M. E.; Oakley, R. T.; Tham, F. S.; Haddon, R. C. *J. Am. Chem. Soc.* **2004**, *126*, 14297–14302.

(23) Huang, L.; Kertesz, M. *J. Am. Chem. Soc.* **2007**, *129*, 1634–1643. Covalent bonding interactions for **1a** based on structural consideration have been discussed in this literature. Similar discussion is also seen in the literature. Chi, X.; Itkis, M. E.; Tham, F. S.; Oakley, R. T.; Cordes, A. W.; Haddon, R. C. *Int. J. Quantum Chem.* **2003**, *95*, 853–865.

(24) Due to the extremely low solubility of **2a**, the monomeric properties of **2a** could not be measured. Therefore the solution absorption band of **2a** was estimated from that of **2b**, which had *tert*-butyl groups on the phenalenyl rings. It is noted that the *tert*-butyl groups effectively prohibit the phenalenyl overlap between the neighboring molecules even in a solid state. See ref 11.

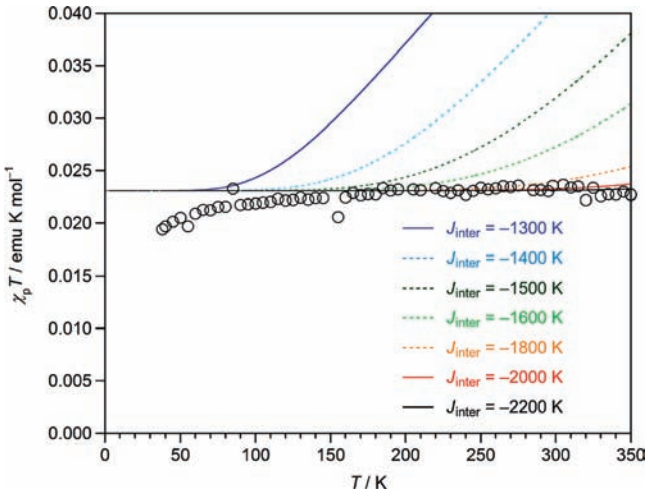

Figure 5. $\chi T-T$ plot of the solid **2a**. Measured data are plotted as open circles. Theoretical curves are drawn using the alternating Heisenberg chain model with the parameters of $J_{intra} = -1200$ K (fixed), $J_{inter} = -1300$ to -2200 K, impurity spin contamination = 6.15%, $g = 2.00$, and diamagnetic susceptibility = -562×10^{-6} emu mol^{-1}.

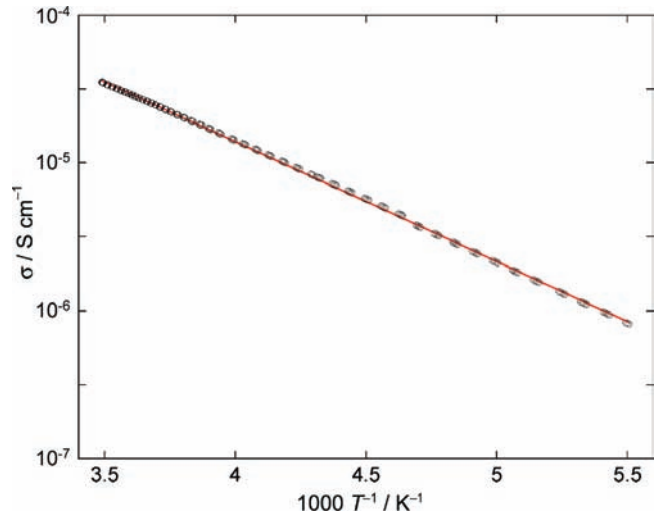

Figure 6. Compressed pellet conductivity of **2a**. The measured data are plotted as open circles and the theoretical line is drawn in red.

on the (0 0 1) surface of the single crystal, gave an extremely lower-energy shifted band centered at 7822 cm^{-1} with respect to the solution absorption band of **2b**, indicating that the intermolecular covalent bonding interaction affects the electronic structure of the molecule in the 1D chain.

It should be noted that the shifted band of **2a** is located at a higher-energy region relative to that of **1a** (6804 cm^{-1}). It has been shown that the 1D chain of **1a** possesses a stronger covalent bonding interaction between the molecules than within the molecule.[23] Extrapolation of this result allows us to presume that the 1D chain of **2a** also has a similar state but with a more enhanced intermolecular covalent bonding interaction, because **2** has larger spin densities on the phenalenyl rings than **1** on the basis of theoretical considerations. The higher-energy band of **2a** relative to that of **1a** can be explained in that the intra- and intermolecular covalent bonding interactions are more unbalanced in strength in the 1D chain of **2a**. The more enhanced bonding alternation causes a greater separation in energy between HOMO and LUMO of the 1D chain. In other words, compared with **1a**, the α-spin electron of **2a** is more localized at one phenalenyl ring while the β-spin electron is more localized at the other (see Figure S2, Supporting Information), and the resulting larger spin densities demand a stronger intermolecular covalent bonding interaction, and consequently more unbalanced covalent bonding interactions afford a larger energy gap between the valence and conduction bands.[25]

Magnetic Measurements. The SQUID measurements of the polycrystals of **2a** showed basically diamagnetic behavior in the temperature range of 30−350 K. Small positive χT values would be derived from a small amount of monoradical impurities. The χT values are almost constant above 100 K (Figure 5), in high contrast to the increasing χT values of **1a** above 200 K.[10a] Huang and Kertesz have theoretically estimated the magnetic interactions of the 1D chain of **1a** using the antiferromagnetic 1D Heisenberg chain model.[23] The theoretical study reveals that the 1D chain of **1a** has relatively balanced interactions; the intramolecular exchange interaction (J_{intra}) of -2300 K and the intermolecular one (J_{inter}) of -3400 K. The negligible spin susceptibility of **2a** indicates that there is too strong a spin−spin pairing interaction in the 1D chain to detect changes in the susceptibility at least up to 350 K, and that the strong interaction would be more negative than -3400 K. In order to estimate the minimum limit of the strong spin−spin interaction, we also used the antiferromagnetic 1D Heisenberg chain model for the 1D chain of **2a**.[26] In the previous work, we have determined the J_{intra} of -1900 K for **2b**, which is in an isolated monomer state (that is, $J_{inter} = 0$) due to the bulky *tert*-butyl groups. On the basis of the discussion on the bond length of *a*, the J_{intra} for **2a** in the 1D chain would be around -1200 K. Using the J_{intra} of -1200 K, we could deduce the J_{inter} of more negative than -2000 K (Figure 5), but a more accurate estimation of the J_{inter} needs further examination with the help of theoretical calculations.

Electroconductive Behavior. In the crystal, **2a** forms a linear conjugation that is made of alternating intra- and intermolecular covalent bonding interactions, and π-electrons could delocalize along the linear 1D chain. We measured electroconductivity of the compressed pellet of the recrystallized **2a** using a two-probe method. The room-temperature conductivity (σ_{rt}) was 5×10^{-5} S·cm^{-1} with an activation energy (E_a) of 0.2 eV at 180−286 K (Figure 6). This semiconductive behavior is similar to that of **1a** ($\sigma_{rt} = 1 \times 10^{-5}$ S cm^{-1}, $E_a = 0.3$ eV) although there is more enhanced bonding alternation in **2a**. In order to estimate the electronic structure in the solid state, we performed a preliminary band structure calculation using the extended Hückel theory (EHT) for the crystal of **2a**.[27,28] The dispersions of valence and conduction bands were found to be very large (0.47 and 0.42 eV, respectively) along the 1D chain (*X*), whereas slight dispersions were also seen along *Y* (Figure 7). The smaller activation energy for **2a** than **1a** would be ascribable to the two-dimensionality of the band structure due to the slight $\pi-\pi$ contact between the 1D chains of **2a** in contrast to the one-

(25) The direction of the transition, which gives direct information about the relative strength of the intra- and intermolecular covalent bonding interactions, could not be determined due to the crystal system with a four-fold screw axis, $I4_1/cd$ (See Figure S1, Supporting Information).

(26) Johnston, D. C.; Kremer, R. K.; Troyer, M.; Wang, X.; Klümper, A.; Bud'ko, S. L.; Panchula, A. F.; Canfield, P. C. *Phys. Rev. B* **2000**, *61*, 9558–9606.

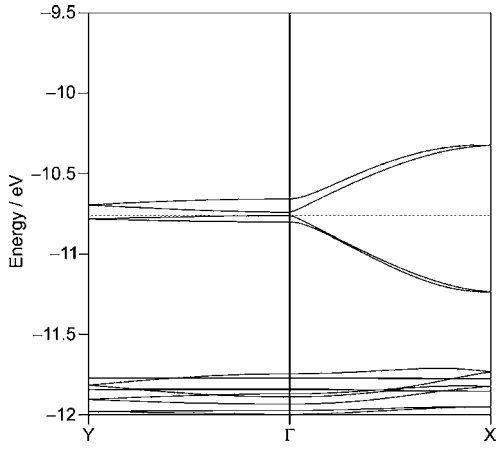

Figure 7. Band structure of **2a** along X ($^1/_2$, 0, 0) and Y (0, $^1/_2$, 0) on a (0 0 1) sheet (layer 1 in Figure S1, Supporting Information). The dotted line represents the Fermi level.

dimensional band structure of **1a**. The dispersion along Z (0, 0, $^1/_2$) should be very small because there is no $\pi-\pi$ contact in its direction.

Conclusion

We have demonstrated that the spin-localizing nature on the phenalenyl rings in the singlet biradical **2a** is relevant to the intermolecular covalent bonding interaction, which dominates the crystal structure to afford the 1D chain. The 1D chain possesses alternating intra- and intermolecular covalent bonding interactions, and the linear conjugation leads to the lower-energy shift in the optical band and to the semiconductive property. The intermolecular covalent bonding interaction is stronger than the intramolecular one, and the bonding alternation is more enhanced in **2a** than **1a**, leading to the wider energy gap of **2a** between the valence and conduction bands.

It is a well-established concept that a covalent bond is a chemical bond that is formed by a pairing of two electrons.[29] Usually, the electron pairing is confined within a single molecule frame to form a closed-shell ground state. However, once the pair is weaken by forming an aromatic sextet, or more generally by rotating a double bond or stretching a σ-bond, the partially unpaired electron demands a second pairing and mostly contributes to a σ-bond formation between molecules with loss of the original pairing. Electron delocalization at the spin-bearing reactive center leads to suppression of the σ-bond formation, and instead, electrons are weakly paired to form a long covalent bonding including multicenter bonding along with partial retention of the original pairing. In this way coexistence of intra- and intermolecular covalent bonding interactions is established in molecular assemblages, being one of the salient features of singlet biradical molecules. The present hydrocarbon-based singlet biradical **2a** also gives a testing ground for the occurrence of multicenter bonding in molecular assemblages and for their role in terms of novel chemical bonding. Alternating covalent bonding interactions based on molecular assemblages will contribute to the quest for exotic genuinely organic molecular functionalities such as purely organic magnetism involving modification of singlet wave functions.[30]

Experimental Section

Materials and Methods. All experiments with moisture- or air-sensitive compounds were performed in anhydrous solvents under an argon atmosphere in well-dried glassware. Dichloromethane, toluene, benzene, and DMF were dried over calcium hydride and distilled prior to use. Ethanol was dried over magnesium ethoxide and distilled prior to use. 2,4,6-Trimethylpyridine was obtained from a commercial source and was used without further purification. Column chromatography was performed with silica gel [Wako gel C-200 (Wako)]. Infrared spectra were recorded on a JASCO FT/IR-660M spectrometer. The electronic absorption spectrum was measured by a Shimadzu UV-3100PC spectrometer. ^{1}H NMR spectra were obtained on JEOL EX-270 spectrometers. FAB mass spectra were taken using JEOL JMS SX-102 mass spectrometers. The polarized reflection spectrum in the infrared and visible regions was observed using two spectrometers combined with a microscope: FT-IR spectrometer Nicolet Magna 760 (600−12000 cm^{-1}) and multichannel detection system Atago Macs 320 (11000−30000 cm^{-1}). Absolute reflectivity was determined by comparing the reflected light from a gold mirror and silicon single crystal, respectively. A single crystal of **2a** was fixed with silicon grease on a copper sample holder, and the crystal face was adjusted so as to be normal to the incident light by use of goniometer head. Temperature-dependent magnetic susceptibility was measured for randomly oriented polycrystalline samples of **2a** on a Quantum Design SQUID magnetometer MPMS-XL with an applied field of 0.1 T in the temperature range of 30−350 K. Below 30 K, the sum of the diamagnetic susceptibilities derived from **2a** and a sample tube is comparable to the paramagnetic susceptibility of monoradical impurities, leading to uncertainty of the magnetic susceptibility measured. Gradual decrease of the χT values below ∼100 K would be explained by the reasons.

7,8,15,16-Tetraphenylfluoratheno[8,9-*k*]fluoranthene (3). The compound **3** was synthesized according to the previously reported procedures.[11,15]

3,11-/3,12-Dibromo-7,8,15,16-tetraphenylfluoratheno[8,9-*k*]fluoranthene (4). To a solution of **3** (2.279 g, 3.35 mmol) in dichloromethane (2000 mL) was added bromine (1.12 g, 7.03 mmol), and the reaction mixture was stirred for 4 h at room temperature. After the addition of aq 10% Na_2SO_3, the organic layer was separated and washed with brine, dried over Na_2SO_4 and filtered, and the solvent was removed *in vacuo*. The dibromo compounds **4** (2.580 g, 92%) were obtained as a vivid yellow powder. Mp >300 °C. TLC R_f 0.76 [hexane/benzene (1:1, v/v)]. ^{1}H NMR (270 MHz, $CDCl_3$) δ 7.69 (d, J = 8.4 Hz, 2H), 7.26 (d, J = 7.9 Hz, 2H), 7.15−6.94 (m, 22H), 5.65 (d, J = 6.9 Hz, 2H), 5.41 (d, J = 7.9 Hz, 2H). FAB MS m/z 836 (M^+). Anal. Calcd for $C_{54}H_{30}Br_2$: C, 77.34; H, 3.61. Found: C, 77.17; H, 3.61.

3,11-/3,12-Bis(2-methoxycarbonylethenyl)-7,8,15,16-tetraphenylfluorantheno[8,9-*k*]fluoranthene (5). A mixture of **4** (2.58 g, 3.08 mmol), $Pd(CH_3CN)_2Cl_2$ (31.5 mg, 0.12 mmol)), Ph_4PCl (277 mg, 0.74 mmol), and AcONa (1.01 g, 12.3 mmol) in DMF (200 mL) was degassed and purged with argon three times. Methyl acrylate (1.66 mL, 18.5 mmol) was added to the mixture, and the mixture was heated to 140 °C for 7.5 h. After cooling, the reaction mixture was filtered and concentrated *in vacuo* to give **5** (2.61 g) as a vivid reddish orange powder. This material was used for the next reaction without further purification. TLC R_f 0.36 (dichloromethane). ^{1}H NMR (270 MHz, $CDCl_3$) δ 8.33 (d, J = 16 Hz, 2H), 7.91 (d, J = 8.2 Hz, 2H), 7.44 (d, J = 7.7 Hz, 2H), 7.25−7.02 (m, 22 H), 6.43

(27) The band structure calculation was performed using the YAeHMOP package, which is freely available on the Web at http://sourceforge.net/projects/yaehmop/.
(28) The band structure calculation based on the EHT is a restricted method, which may not be appropriate for singlet biradical species. Instead, a calculation including an adequate electron−electron correlation may give proper results.
(29) Pauling, L. *The Nature of the Chemical Bond*, 3rd ed.; Cornell University: Ithaca, NY, 1960.
(30) Shiomi, D.; Sato, K.; Takui, T. *J. Phys. Chem. B* **2001**, *105*, 2932–2938.

(d, $J = 16$ Hz, 2H), 5.74 (d, $J = 7.1$ Hz, 2H), 5.70 (d, $J = 7.7$ Hz, 2H), 3.79 (s, 6H). FAB MS m/z 849 ($[M+H]^+$). IR (KBr) 1706 cm^{-1}.

3,11-/3,12-Bis(2-methoxycarbonylethyl)-7,8,15,16-tetraphenylfluorantheno[8,9-*k*]fluoranthene (6). A mixture of **5** (2.61 g, 3.08 mmol), zinc powder (10.0 g, 154 mmol), acetic acid (260 mL), and toluene (260 mL) was refluxed for 41 h. After cooling, the reaction mixture was filtered. The filtrate was washed with saturated aqueous $NaHCO_3$ and brine, dried over Na_2SO_4, and filtered. After column chromatography on silica gel (dichloromethane), **6** (1.87 g, 71%, 2 steps) was obtained as a vivid yellow powder. Mp 273.0−285.5 °C. TLC R_f 0.38 (dichloromethane). ^{1}H NMR (270 MHz, $CDCl_3$) δ 7.71 (d, $J = 8.2$ Hz, 2H), 7.23−7.03 (m, 22 H), 6.94 (d, $J = 7.4$ Hz, 2H), 5.71, 5.70 (d, $J = 7.2$ Hz, 2H), 5.62, 5.61 (d, $J = 7.4$ Hz, 2H), 3.62 (s, 6H), 3.28 (d, $J = 7.9$ Hz, 4H), 2.63 (d, $J = 7.9$ Hz, 4H). FAB MS m/z 853 ($[M+H]^+$). IR (KBr) 1739 cm^{-1}. Anal. Calcd for $C_{62}H_{44}O_4$: C, 87.30; H, 5.20. Found: C, 86.92; H, 5.07.

3,11-/3,12-Bis(2-carboxyethyl)-7,8,15,16-tetraphenylfluorantheno[8,9-*k*]fluoranthene (7). A mixture of **6** (563 mg, 0.659 mmol), lithium iodide (1.77 g, 13.2 mmol), and 2,4,6-trimethylpyridine (55 mL) was heated to 185 °C for 3 h. After cooling, the reaction mixture was concentrated *in vacuo*, and 2 M hydrochloric acid was added. The solid was collected and washed with water to give **7** (551 mg) as a deep yellow powder. This material was used for the next reaction without further purification. Mp >300 °C. ^{1}H NMR (270 MHz, DMSO-d_6) δ 7.82 (d, $J = 8.4$ Hz, 2H), 7.25−7.04 (m, 22 H), 6.97 (d, $J = 7.6$ Hz, 2H), 5.51, 5.50 (d, $J = 7.2$ Hz, 2H), 5.41, 5.40 (d, $J = 7.6$ Hz, 2H), 3.17 (t, $J = 7.2$ Hz, 4H), 2.51 (t, $J = 7.2$ Hz, 4H). FAB-MS m/z 825 ($[M+H]^+$). IR (KBr) 3414, 1704 cm^{-1}.

1,2,3,10,11,12-Hexahydro-1,10-/1,12-dioxo-6,7,15,16-tetraphenyldicyclopenta[*b*,*g*]naphthaleno[1,2,3-*cd*;6,7,8-*c*′*d*′]diphenalene (8). A mixture of **7** (551 mg, 0.659 mmol) and oxalyl chloride (30 mL) was refluxed for 2 h. The reaction mixture was cooled and concentrated *in vacuo*. The resulting solid was dissolved in dichloromethane (55 mL) and was cooled to −78 °C. Aluminum chloride (464 mg, 3.48 mmol) was added, and the reaction mixture was allowed to warm to −30 °C over 2.5 h. After the reaction mixture was poured into ice-cold water, 2 M hydrochloric acid was added, and the organic layer was separated. The aqueous layer was extracted with dichloromethane. The combined organic layer was washed with saturated aqueous $NaHCO_3$ and brine, dried over Na_2SO_4, and filtered. After column chromatography on silica gel (dichloromethane), **8** (369 mg, 71%, 2 steps) was obtained as a vivid orange powder. Mp >300 °C. TLC R_f 0.69 [hexane/ethyl acetate (1:1, v/v)]. ^{1}H NMR (270 MHz, $CDCl_3$) δ 7.75 (d, $J = 7.6$ Hz, 2H), 7.25−7.00 (m, 22 H), 5.78, 5.77 (d, $J = 7.6$ Hz, 2H), 5.66, 5.65 (d, $J = 7.3$ Hz, 2H), 3.30 (t, $J = 6.8$ Hz, 4H), 2.88 (t, $J = 6.8$ Hz, 4H). FAB MS m/z 789 ($[M+H]^+$). IR (KBr) 1685 cm^{-1}. Anal. Calcd for $C_{60}H_{36}O_2$: C, 91.34; H, 4.60. Found: C, 91.01; H, 4.56.

1,2,3,10,11,12-Hexahydro-1,10-/1,12-dihydroxy-6,7,15,16-tetraphenyldicyclopenta[*b*,*g*]naphthaleno[1,2,3-*cd*;6,7,8-*c*′*d*′]diphenalene (9). A mixture of **8** (339 mg, 0.43 mmol), sodium boron hydride (48.8 mg, 1.29 mmol), and dichloromethane (80 mL) and ethanol (32 mL) was stirred for 1.5 h at room temperature. Sodium boron hydride (32.5 mg, 0.86 mmol) was added to the reaction mixture, and the mixture was stirred for an additional 1.5 h at room temperature. After addition of water and 2 M HCl, the organic layer was separated, and the aqueous layer was extracted with dichloromethane. The combined organic layer was washed with saturated aqueous $NaHCO_3$ and brine, dried over Na_2SO_4, and filtered to give **9** (355 mg, 100%) as a vivid orange powder. Mp >300 °C. TLC R_f 0.58 [dichloromethane/ethyl acetate (1:1, v/v)]. ^{1}H NMR (270 MHz, $CDCl_3$) δ 7.23−7.03 (m, 22 H), 6.88 (d, $J = 7.3$ Hz, 2H), 5.67 (d, $J = 7.3$ Hz, 2H), 4.96 (m, 1H), 3.21−3.07 (m, 2H), 2.97−2.84 (m, 2H), 2.25−2.00 (m, 4H), 1.67, 1.65 (s, 2H). FAB MS m/z 792 (M^+). IR (KBr) 3434 cm^{-1}. Anal. Calcd for $C_{60}H_{40}O_2$: C, 90.88; H, 5.08. Found: C, 90.84; H, 5.17.

1,10-/1,12-Dihydro-6,7,15,16-tetraphenyldicyclopenta[*b*,*g*]naphthaleno[1,2,3-*cd*;6,7,8-*c*′*d*′]diphenalene (10). To a solution of **9** (100 mg, 0.126 mmol) in toluene (50 mL) heated to 90 °C, a catalytic amount of *p*-toluenesulfonic acid monohydrate was added, and the reaction mixture was heated at 90 °C for 30 min. The mixture was cooled in an ice-bath. The crude product was purified by column chromatography on silica gel (toluene) to give **10** (83.0 mg, 87%) as an air-sensitive dark yellowish brown powder. TLC R_f 0.36 [hexane/benzene (2:1, v/v)]. ^{1}H NMR (270 MHz, $CDCl_3$) δ 7.20−7.05 (m, 20 H), 6.95 (dt, $J = 7.6$, 1.9 Hz, 2H), 6.71 (d, $J = 7.3$ Hz, 2H), 6.62 (dt, $J = 9.9$, 2.2 Hz, 2H), 6.10 (dt, $J = 9.9$, 4.0 Hz, 2H), 5.68 (d, $J = 7.6$ Hz, 2H), 5.63 (d, $J = 7.3$ Hz, 2H), 3.84−3.77 (m, 4H). FAB MS m/z 756 (M^+).

6,7,15,16-Tetraphenyldicyclopenta[*b*,*g*]naphthaleno[1,2,3-*cd*;6,7,8-*c*′*d*′]diphenalene (2a). To a solution of **10** (83.0 mg, 0.110 mmol) in benzene (80 mL) heated at 80 °C, a solution of *p*-chloranil (29.7 mg, 0.121 mmol) in benzene (10 mL) was added. The reaction mixture was slowly cooled to room temperature, and the resulting crystals were collected and washed with acetone to give **2a** (68.6 mg, 83%) as dark purple plates. Mp >300 °C (in a sealed tube). TLC R_f 0.55 [hexane/benzene (1:1, v/v)]. FAB MS m/z 755 ($[M+H]^+$). Anal. Calcd for $C_{60}H_{34}$: C, 95.46; H, 4.54. Found: C, 95.15; H, 4.73.

Computational Methods. DFT calculations were performed with the Gaussian 03 program.[31] All geometry optimizations were carried out at the B3LYP level of density functional theory with the 6-31G** basis set. Singlet biradical character was estimated using a CASSCF(2,2) method in the RB3LYP optimized geometry, and using a broken-symmetry UB3LYP/6-31G** method along with geometry optimization. A band structure calculation was performed with an extended HMO method using the YAeHMOP package[27] in the X-ray crystallographic geometry.

Crystal Data for 2b. $C_{60}H_{34}$, $M = 754.87$, tetragonal, space group $I4_1/cd$, $a = 12.4649(5)$ Å, $c = 47.8243(16)$ Å, $V = 7430.6(5)$ Å^3, $Z = 8$, μ(Mo Kα) = 0.077 cm^{-1}, $\rho_{calcd} = 1.350$ g cm^{-3}, $T = 200$ K, $R1(wR2) = 0.067$ (0.160) for 272 parameters and 2490 unique reflections with $I > 2\sigma(I)$, GOF = 1.06. Data collection for X-ray crystal analysis was performed on Rigaku/Varimax diffractometer (Mo Kα, $\lambda = 0.710\,69$ Å). The structure was solved with direct methods and refined with full-matrix least-squares.

Acknowledgment. This work was supported in part by Yamada Science Foundation (T.K.), the Grants-in-Aid for Scientific Research on Innovative Areas (No. 2105, T.K.), Grants-in-Aid for Scientific Research (No. 18350007, M.N.) from the Ministry of Education, Culture, Sports, Science and Technology of Japan, PRESTO-JST (Y.M. and D.S.), CREST-JST (K.S. and T.T.), and the Global COE program "Global Education and Research Center for Bio-Environmental Chemistry" of Osaka University (A.S.). A.S. acknowledges the JSPS Fellowship for Young Scientists.

Supporting Information Available: Crystal packing of **2a**, HOMOs of α-spin and β-spin electrons for **2** calculated with a broken-symmetry UB3LYP method, input files for the Gaussian calculation, details of crystallographic data collection and structure refinement, tables of atomic coordinates, bond distances and angles, and isotropic thermal parameters in CIF format, and complete ref 31. This material is available free of charge via the Internet at http://pubs.acs.org.

JA1037287

(31) Frisch, M. J.; et al. *Gaussian 03*, revision D.01; Gaussian, Inc.: Wallingford, CT, 2004.